

# LIGAND OF CADMIUM (II)

66

AFFAIL 8

# Abstract.

Nowadays, the synthesis of metal complexes containing ligands with N, and O-donor centers have particular importance. The research solves the problem of competitive coordination in coordination chemistry are very important to introduce these complexes into practice as fluorescent, antimicrobial, fungicide, herbicides, and biostimulators in agriculture.

It is necessary to conduct systematic work on the synthesis of new complex compounds of phenanthroline with similar properties.

# **Key words:**

1,10-phenanthroline (Phen), acetic acid, crystal structure, H-bond energy, Hirshfeld surface.

### Introduction.

The coordination chemistry has a special interest in all biologically active metal ions forming metal complexes, and the large number of phenantroline complex compounds obtained with metals [1,2]. Coordination complexes are compounds formed between a metal ion and a ligand. Metal ions are essentially Lewis acids, and ligands are similar to Lewis bases. In most cases, the donor atoms of the ligand have an unpaired electron pair, which donates an electron pair to the empty d-orbitals in the metal, forming a Lewis acid-base complex [3]. 1,10-phenanthroline is a heterocyclic compound that is one of the most popular bidentate N, N-chelating agents used in coordination chemistry. Metal complexes formed by 1,10-phenanthroline with metal cations have photochemical and photophysical properties. 1,10-phenanthroline is biologically active, so it is interesting to study the biological effects of its complexes [4]. At the same time, cadmium applied as a barrier to nuclear fission in television screens, lasers, batteries, paint pigments, cosmetics, and galvanizing steel is used [5]. Crystal structures of mixed ligand complexes containing cadmium dithiocarbamates and nitrogen-containing bases such as 2,2'-bipyridine, 1,10-phenanthroline, and tetramethylethylenediamine have been reported [6]. Cadmium cycling and immobilization in the environment and some organisms need a number of analytical techniques (such as ligand exchange chromatography) that significantly depends on the complex structure of the metal center by chelating nitrogen donor ligands. The Schiff bases have been used as chelating agents in coordination chemistry. It is known that N and O atoms play a key role in the coordination of metals in the active sites of many metal-containing biomolecules. The Schiff base metal complexes have been widely studied because of their industrial, antifungal, antibacterial, anticancer, antiviral, and herbicidal applications [7].

The aim of this work is the synthesis and study of a new metal complex based on 1,10-phenanthroline and cadmium (II) ions.

# Methods va materials.

All reagents were obtained from commercial sources and used without purification. Determination of the crystal structure was carried out using a CCD diffractometer (Oxford diffraction Xcalibur-R (CuKa, - radiation, λ=1.54184 Å,  $\omega$  - scanning mode, graphite monochromator (at 293K))

The hydrogen bond geometry of the complex and the value of some bond lengths and angles are presented in Tables 1 and 2. The structure was determined using the SHELX-97 software package [9]. Molecular drawings were obtained by the MERCURY software package [10].

Of phenanthroline-based synthesized mixed-ligand complex compound Raman spectrometer, "HORIBA Scientific" № MM5302723017A00163 in the spectrometer in the range of 0-4000 cm<sup>-1</sup>, Termiz State University, Faculty of Chemistry, It was detected in the device at the scientific laboratory.

IR-spectrum of complex compounds synthesized based on phenanthroline, IRTracer 100 IR Furye (Shimadszu, Japan) In a spectrometer, the IR spectrum of the complex compound is in the range of 400-4000 cm<sup>-1</sup> Tashkent Scientific Research Institute of Chemical Technology, detected in the device at the scientific laboratory.

Synthesis of the complex compound.

0.26653 g (1 mol) and 0.36042 g (2 mol) of 1.10-phenanthroline were dissolved from cadmium (II) acetate (Cd(CH,COO), 2H,O) in water and ethyl alcohol, respectively, and 1:2 ratio solutions were used under stirring. The resulting precipitate was dissolved using 2 drops of dilute acetic acid. Then, it was intensively mixed at 60 <sup>o</sup>C for 40 minutes using a magnetic stirrer. The solution was left at room temperature. As a result, after 15 days, it was observed that a colorless transparent complex compound crystal grew at the bottom of the container. When crystals suitable for RTT analysis were isolated and examined.

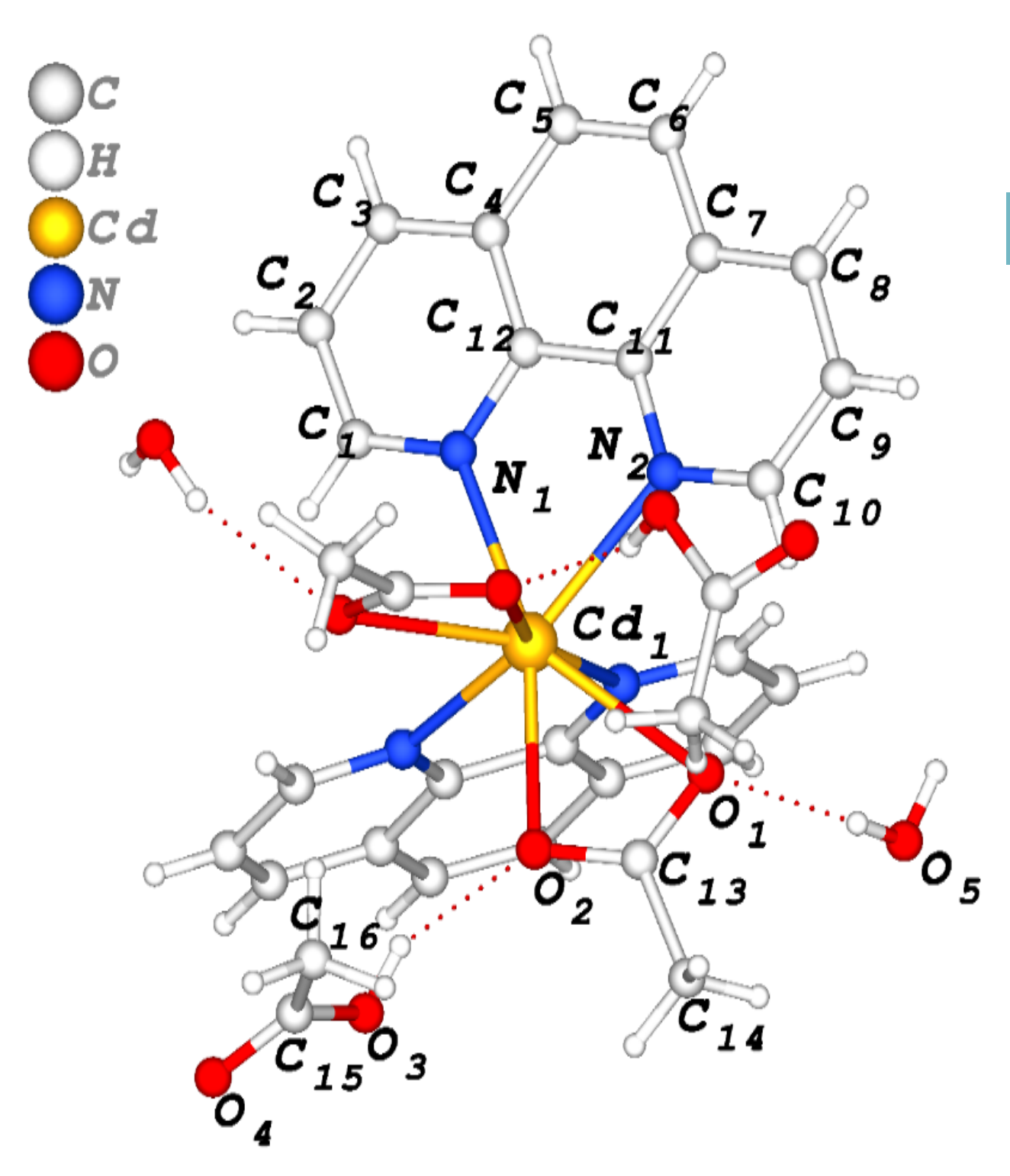
The yield of the reaction is 75%. C32H34CdN4O10 (Mr=747.0442 g/mol). Elemental analysis theoretical: C, 51.45; H, 4.59; Cd, 15.05; N, 7.50; O 21.42%, experimental: C, 51.44; H, 4.6; Cd, 15.1; N, 7.45; O, 21.42%.

The reaction equation is as follows.

Figure 1. [(CH,COO),(C1,HgN,),Cd](2CH,COOH·2H,O) synthesis of the complex.

(Acetato $k^2O,O'$ ) bis (1,10-phenan-Bis throline-k<sup>2</sup>N,N') cadmium (II) dihydrate [(CH-<sub>3</sub>COO)<sub>2</sub>(C<sub>12</sub>H<sub>8</sub>N<sub>2</sub>)<sub>2</sub>Cd](CH<sub>3</sub>COOH)<sub>2</sub>·2H<sub>2</sub>O The complex compound is monoclinic, and the parameters of the crystal cell: space group C2/c, a= 22.0322(11)Å, b= 10.3367(3) Å, c=18.7511(9)Å, a= 900, b=127.538(7)°, y= 900 V=3386.2(4) Å<sup>3</sup>, Z=4, T=293 K.

The polyhedron around Cd is octahedron: bonds are equal Cd1-O1 2.624(5) Å, Cd-O2 2.391(5) Å, Cd1-N1 2.428(5) Å, Cd1-N 2.423(4) Å; bond angle are O1-Cd1-O2 51.07(18) (°), O1-Cd1-N1 147.96(15) (°), O1-Cd1-N2 81.41(16)(°) (Table 2).



 $Figure \ 2. \ Molecular \ structure \ of \ the \ complex \ [(CH_3COO)_2(C_{12}H_8N_2)_2Cd] (2\cdot CH_3COOH \cdot 2H_2O). \ The \ dotted$ 

### lines represent hydrogen bonding.

Table 1. Hydrogen bond geometry

D-H··· Å	D-H,Å	H···A,Å	D···A,Å	D-HA, (°)
O3H3AO2	0.8200	1.8900	2.646(11)	153.00
O5H5AO1	0.8500	2.1000	2.921(9)	161.00
O5H5BO4	0.8500	2.0900	2.938(11)	174.00
C10H10O1	0.9300	2.5200	3.197(8)	130.00

Table 2. Some bond lengths and angles of the [(CH<sub>2</sub>COO)<sub>2</sub>(C<sub>12</sub>H<sub>2</sub>N<sub>2</sub>)<sub>2</sub>Cd](CH<sub>2</sub>COOH·2H<sub>2</sub>O) complex.

	$[(CH_3COO)_2(C_{12}H_8H_2)_2Cd](CH_3COOH 2H_2O) \text{ conspicts.}$					
	Bond lengths	(Å)	Bond angles	(°)		
1	Cd1 -O1	2.624(5)	O1 -Cd1 -O2	51.07(18)		
2	Cd1 -O2	2.391(5)	O1 -Cd1 -N1	147.96(15)		
3	Cd1 -N1	2.428(5)	O1 -Cd1 -N2	81.41(16)		
4	Cd1 -N2	2.423(4)	O1 -Cd1 -O1_a	125.11(14)		
5	Cd1 -O1_a	2.624(5)	O1 -Cd1 -O2_a	85.92(19)		
6	Cd1 -O2_a	2.391(5)	O1 -Cd1 -N1_a	79.79(16)		
7	Cd1 -N1_a	2.428(5)	O1 -Cd1 -N2_a	115.57(16)		
8	Cd1 -N2_a	2.423(4)	O2 -Cd1 -N1	160.89(19)		
9	C7 -C8	1.393(9)	O2 -Cd1 -N2	129.77(17)		
10	C8 -C9	1.355(11)	O1_a -Cd1 -O2	85.92(19)		
11	C9 -C10	1.396(9)	O2 -Cd1 -O2_a	81.28(18)		
12	C11 -C12	1.446(9)	O2 -Cd1 -N1_a	99.13(18)		
13	C13 -C14	1.499(11)	O2 -Cd1 -N2_a	79.93(15)		
14	C1 -H1	0.9300	N1 -Cd1 -N2	68.57(16)		
15	C2 -H2	0.9300	O1_a -Cd1 -N1	79.79(16)		

### **Results and Discussion**

The molecular structure of the single crystal  $[(CH_3COO)_2(C_{12}H_8N_2)_2Cd](2CH_3COOH\cdot 2H_2O)$  complex was determined by single crystal X-ray diffraction analysis. To describe the nature of intermolecular interactions (b), the Hirschfeld surface was analyzed using Crystal Explorer17.5 [11] software (Fig. 3, 4).

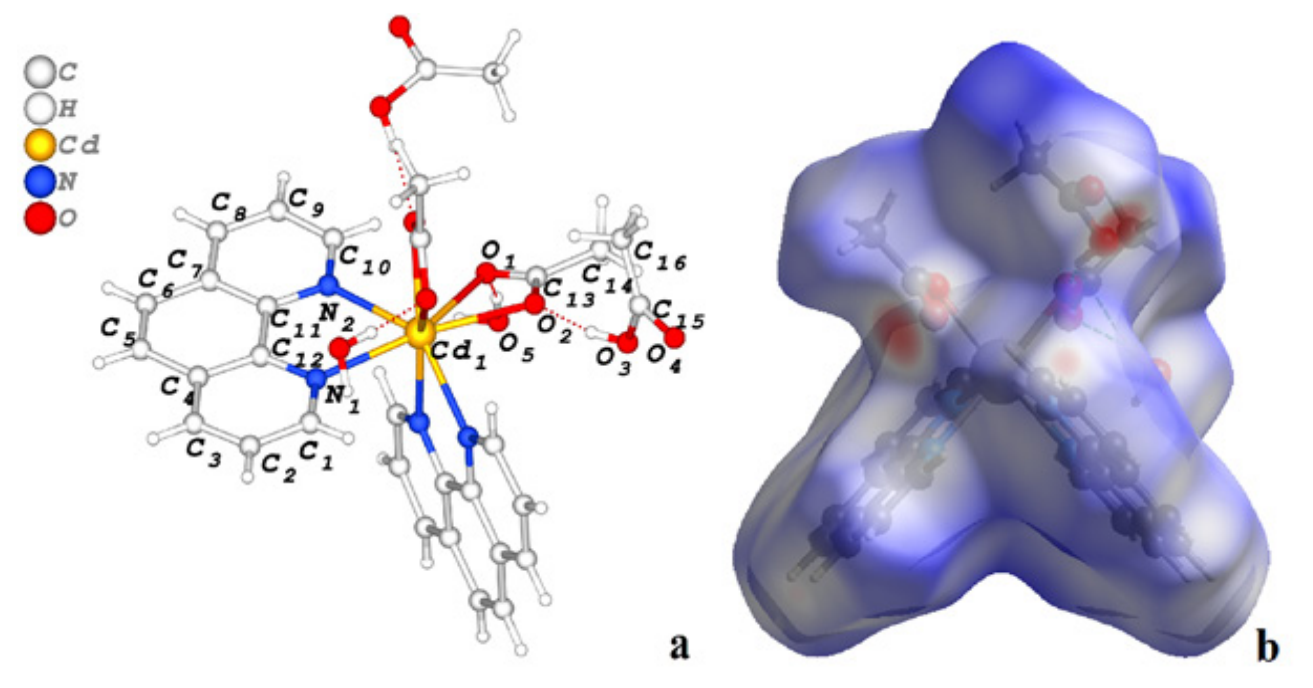


Figure 3: Molecular structure of a single crystal of [(CH\_3COO)\_2(C\_{12}H\_8N\_2)\_2Cd](2CH\_3COOH \cdot 2H\_2O) complex (a), Hirshfeld surfaces (b)

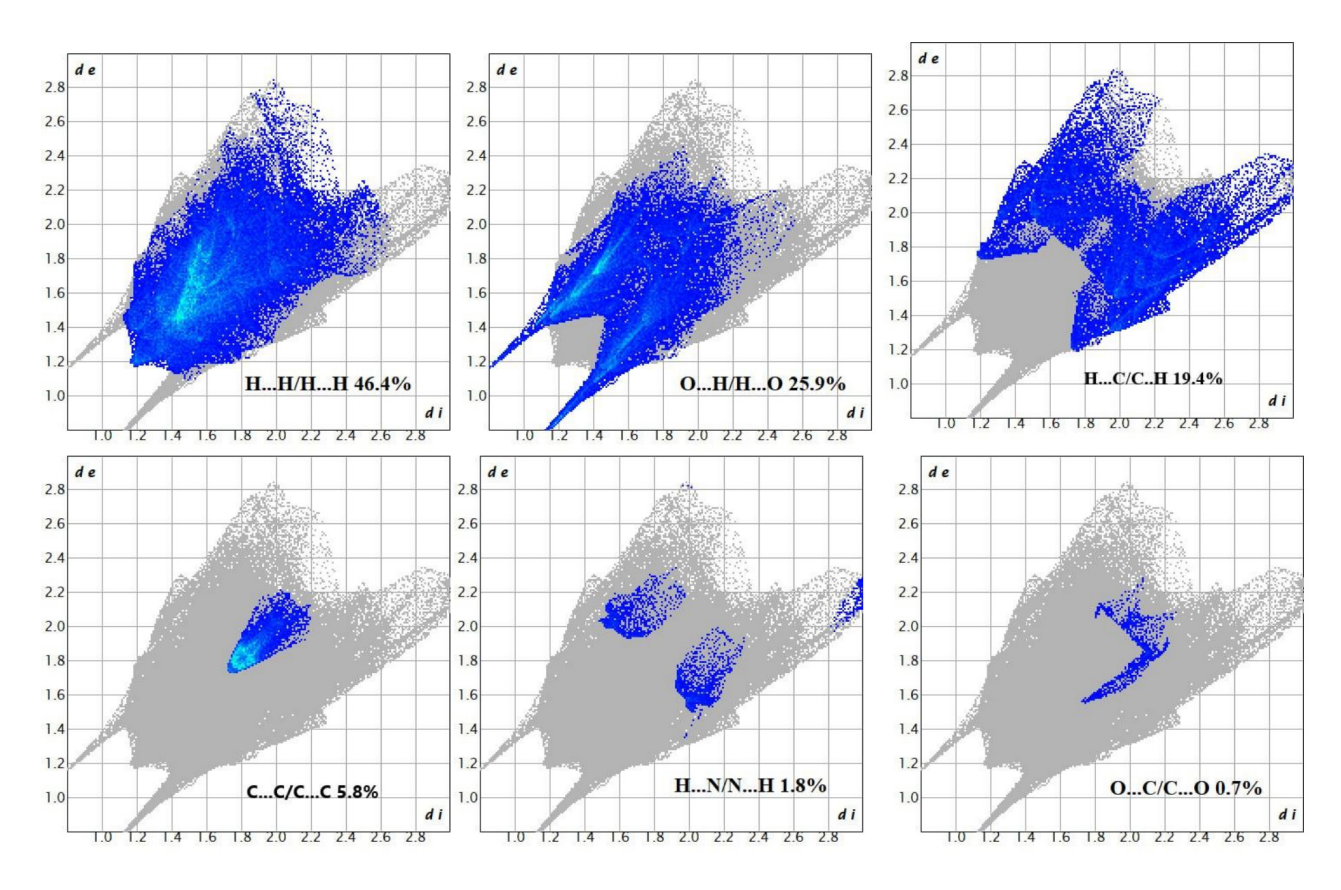


Figure 4: 2D Hirschfeld fingerprint graphic

Figure 3b shows the Hirschfeld surfaces of  $[(CH_3COO)_2(C_{12}H_8N_2)_2Cd]$  ( $2CH_3COOH\cdot 2H_2O$ ) complex single crystal , with red part representing the closest interactions and blue part representing the farthest interactions. Figure 4 shows two-di-

mensional fingerprint plots obtained using the  $d_e$  and  $d_i$ functions, which are showed the contribution of individual interactions to the formation of crystal packing. Thus, Hirschfeld surface analysis indicates on H...H (46.4%), O...H/H...O (25.9%), H...C/C...H (19.4%), C...C (5.8%), H...N /N..H (1.8%), O...C/C...O (0.7%), interactions that are the main contributors to the crystal packing. So, as can be seen from the Hirschfeld surface analysis, the main part of interactions is H...H (46.4%). O...H/H...O (25.9%), and H...C/C...H (19.4%). Quantizing the fundamental energy is one of the best ways to understand the topology of interactions between

molecules in a crystal. This method allows the calculation and comparison of different energy components, i.e. repulsion (Erep), electric (Eele), dispersion (Edis), polarization (<sup>E</sup>pol), and total based on the anisotropy of the topology of pairwise intermolecular interaction energies. Etot () energies. Khatri Fock (HF) function creates new wave functions using the DFT method based on HF/3-21G defined by the molecular cluster environment and is used to calculate the energy range of the obtained compound [12].

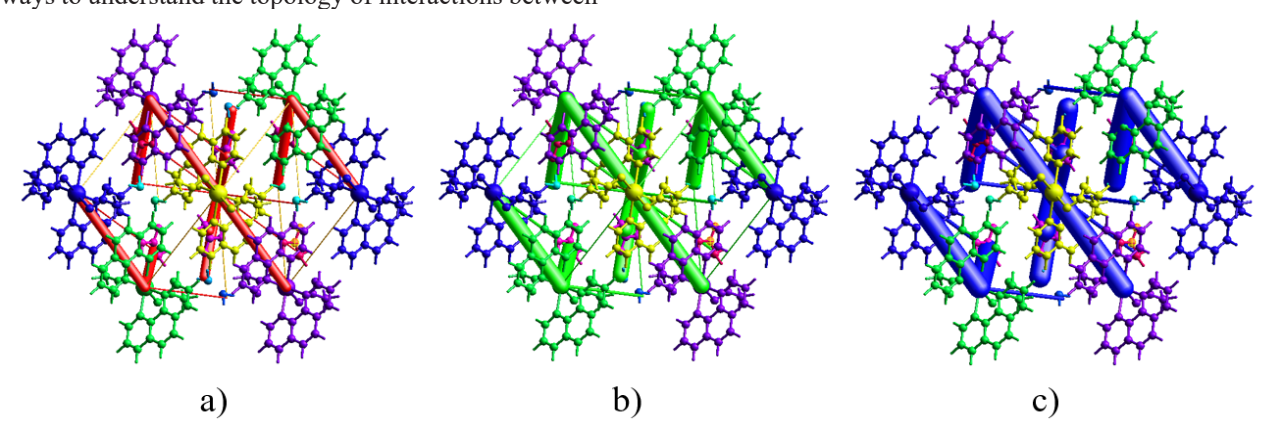


Figure 5. The energy range of complex molecules viewed along [001]: (a) electrostatic, (b) dispersion, (c) total energy force diagram

Fig.5 demonstrates the thickness of the radius of the cylinder indicating the degree of interaction of the energy quantities and the stability of the crystal structure [13]. To avoid the separation of less important interaction energy, we fitted all energy components to cylindrical shapes with a value of 5 kJ/mol, scaled by a scale factor of 80.

Table 3. Color-coded, symmetry case (Symop) and interaction details (R) molecular distances of complex molecules viewed along [001] A.

N	Symop	R	E <sub>ele</sub>	E <sub>pol</sub>	E <sub>dis</sub>	E <sub>rep</sub>	E <sub>tot</sub>
2	-x+1/2, -y+1/2, -z	9.24	-48.4	-14.8	-85.9	41.2	-102.9
2	-	7.52	0.0	nan	0.0	0.0	nan
2	-x, -y, -z	11.44	5.4	-1.1	-7.0	0.2	-1.4
2	x, y, z	10.34	-7.8	-3.1	-17.0	6.9	-19.7
2	-	9.31	0.0	nan	0.0	0.0	nan
2	-	6.72	2.4	-0.3	-1.4	0.0	1.0
2	-x, -y, -z	10.11	0.0	0.0	0.0	0.0	0.0
2	-	4.98	2.9	-1.1	-3.8	0.0	-1.2
2	-	8.64	-7.8	-3.1	-17.0	6.9	-19.7
2	-	7.48	-48.4	-14.8	-85.9	41.2	-102.9
2	-	8.36	5.4	-1.1	-7.0	0.2	-1.4
4	x+1/2, y+1/2, z	12.17	2.9	-1.1	-3.8	0.0	-1.2
2	-x+1/2, -y+1/2, -z	12.79	5.2	-1.3	-2.3	0.0	2.4
2	-	5.90	-48.4	-14.8	-85.9	41.2	-102.9
2	-	6.48	2.9	-1.1	-3.8	0.0	-1.2
2	-	8.26	-7.8	-3.1	-17.0	6.9	-19.7
			-126.3	-59.57	-337.8	144.5	-372.8

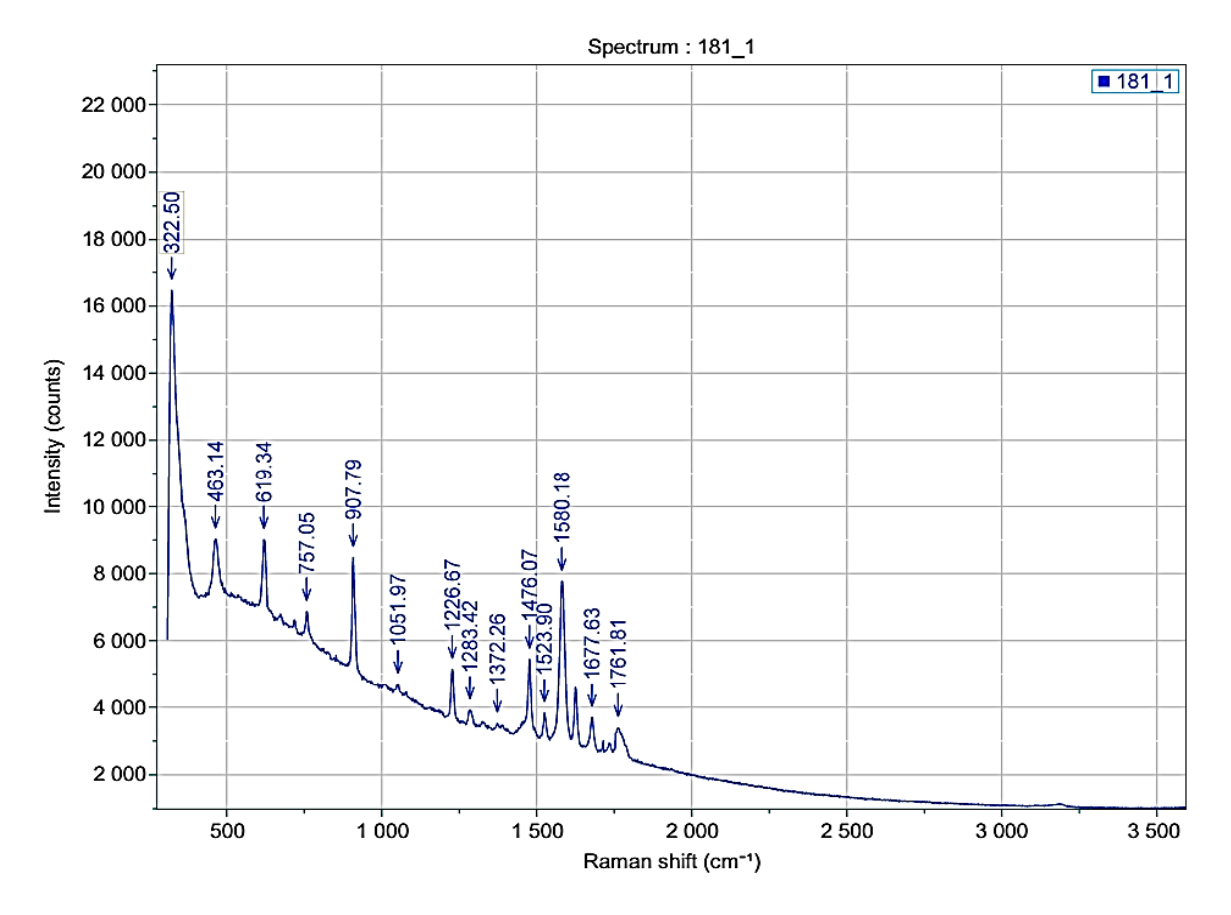
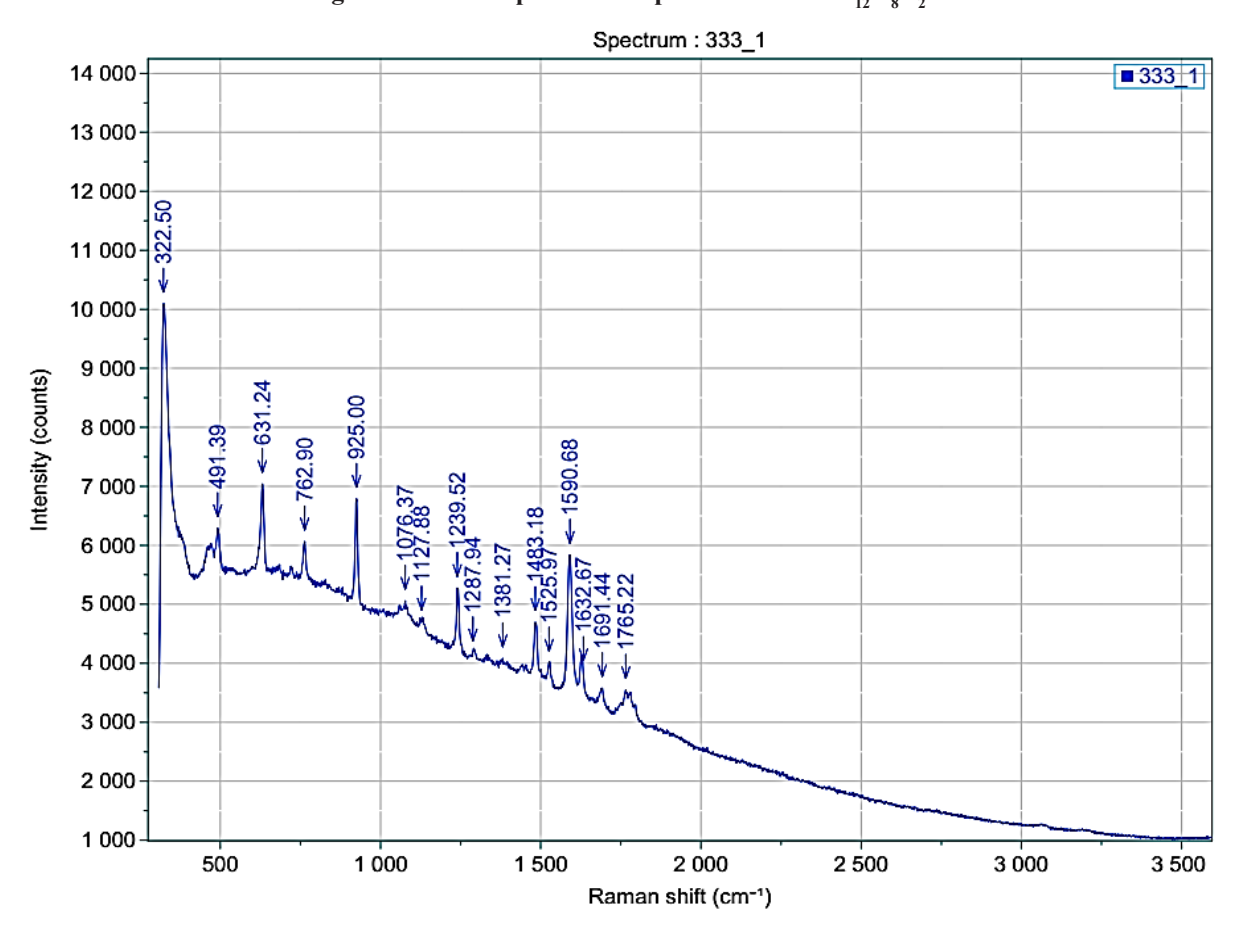


Figure 6. Raman spectrum of phenanthroline  $C_{12}H_8N_2$ .



181 90 %T 80 70 60 1421,54 50 40 30 20 3000 750 3500 2500 2000 1750 1500 1250 1000 4000 cm-1

Figure 7. Raman spectrum of [(CH,COO),(C,H,N,),Cd](2·CH,COOH·2H,O) complex



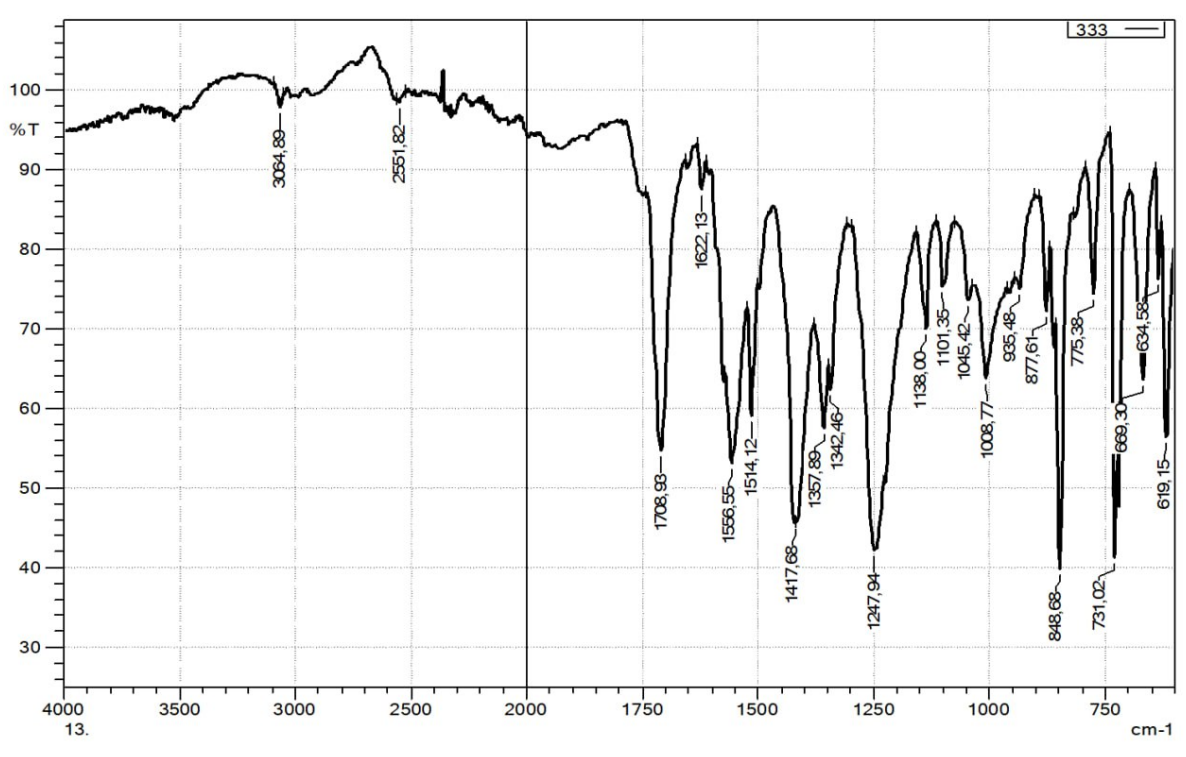


Figure 8. IR spectra of the complex [(CH<sub>3</sub>COO)<sub>2</sub>(C<sub>1</sub>,H<sub>8</sub>N<sub>2</sub>)<sub>2</sub>Cd](2·CH<sub>3</sub>COOH·2H<sub>2</sub>O)

Raman spectra can also provide the information about molecular structure. Electromagnetic radiation field and molecular induce dipole moment are the source of Raman spectra. And the spectra arise from the symmetric vibration of the symmetric bond. IR spectra, however, are attributed to the changes of molecular dipole moment. The two spectra comple-

ment and support each other [14]. The combination of Raman spectra and IR spectra is a powerful method for characterizing the complexes. [15]. The Raman spectra of the complex and 1,10-phenanthroline is shown in Figures 4 and 5. The COO- group stretching vibrations in acetic acid have been assigned to the strong Raman bands at 1512 and 1483 cm<sup>-1</sup>,

respectively. In the complex, however, the COO– group stretching vibrations are at 1590 and 1483 cm<sup>-1</sup>. The separation between them,  $\Delta v - v_{as}$  (COO–)– $v_s$ (COO–)–117 cm<sup>-1</sup>, is indicative of bidendate chelating coordination. This result is complementary to their IR spectra. The bands at 1645, 1616, 1587 and 1560 cm<sup>-1</sup> in the Raman spectra of phen have been assigned to the phenyl ring stretching vibration, which shift to higher frequency of 1653, 1627, 1604 and 1585 cm<sup>-1</sup> in the complex. These may be owing to the coordination of the two nitrogens of phen with the metall ion, as discussed in the IR spectra above. In the complex, the bands at 491 and 631 cm<sup>-1</sup> can be assigned to the Cd-O, Cd-N, stretching vibration, respectively.

Thermogravimetric analysis (TGA) is a suitable method to evaluate the thermal stability as well as to confirm the structural composition of the investigated complexes. This can provide information about a physical and chemical phenomenon caused by a gradual increase in temperature, such as degradation. These properties can be determined, for example, by detecting complex weight changes with temperature or time [16]. Thermal analysis for the complexes was performed under argon in the temperature range of 30-600 °C. The thermogram in Fig. 5 shows the decomposition process of the complex. The thermogram shows multistage degradation of the complexes, the experimental mass loss as a function of the temperature change, and the theoretical mass

loss of the assigned fragment are shown in Fig. 5. As a result of studying the stages of decomposition, it can be concluded that the number of stages mainly corresponds to the number of ligand groups that can be gradually lost. In Figure 3, it was found that the water molecule and the anion (chloride) organic molecule were lost at temperatures lower than the decomposition or loss of the phenanthroline ligand [17].

The derivatogram of the sample [(CH<sub>3</sub>COO)<sub>2</sub>(C<sub>12</sub>H<sub>8</sub>N<sub>2</sub>)<sub>2</sub>Cd] (2CH<sub>3</sub>COOH·2H<sub>2</sub>O) complex is given in Figure 9, which consists of 2 curves.

In the derivative thermogravimetric analysis (DTA) curve, three exothermic effects were detected at 76.4°C, 122.85°C, and 273.63°C, but no endothermic effect was observed. Analysis of the thermogravimetry (TGA) curve shows four intense decomposition temperatures. The first decomposition interval occurred in the temperature range of 37.22–84.58°C, with a mass loss of 0.521 mg or 8.035%. The second decomposition interval was observed at temperatures of 84.58–133.30°C, and it was determined that 0.922 mg or 14.220% of mass was lost. The third interval occurred in the temperature range of 225.32–352.79°C, with a mass loss of 2.462 mg or 37.970%. The fourth decomposition interval was observed at temperatures of 352.79–571.75°C, and it was determined that 0.542 mg or 8.359% of mass was lost. In the temperature range of 37.22–571.75°C, the total mass loss was found to be 4.429 mg, occurring over 65.99 minutes.

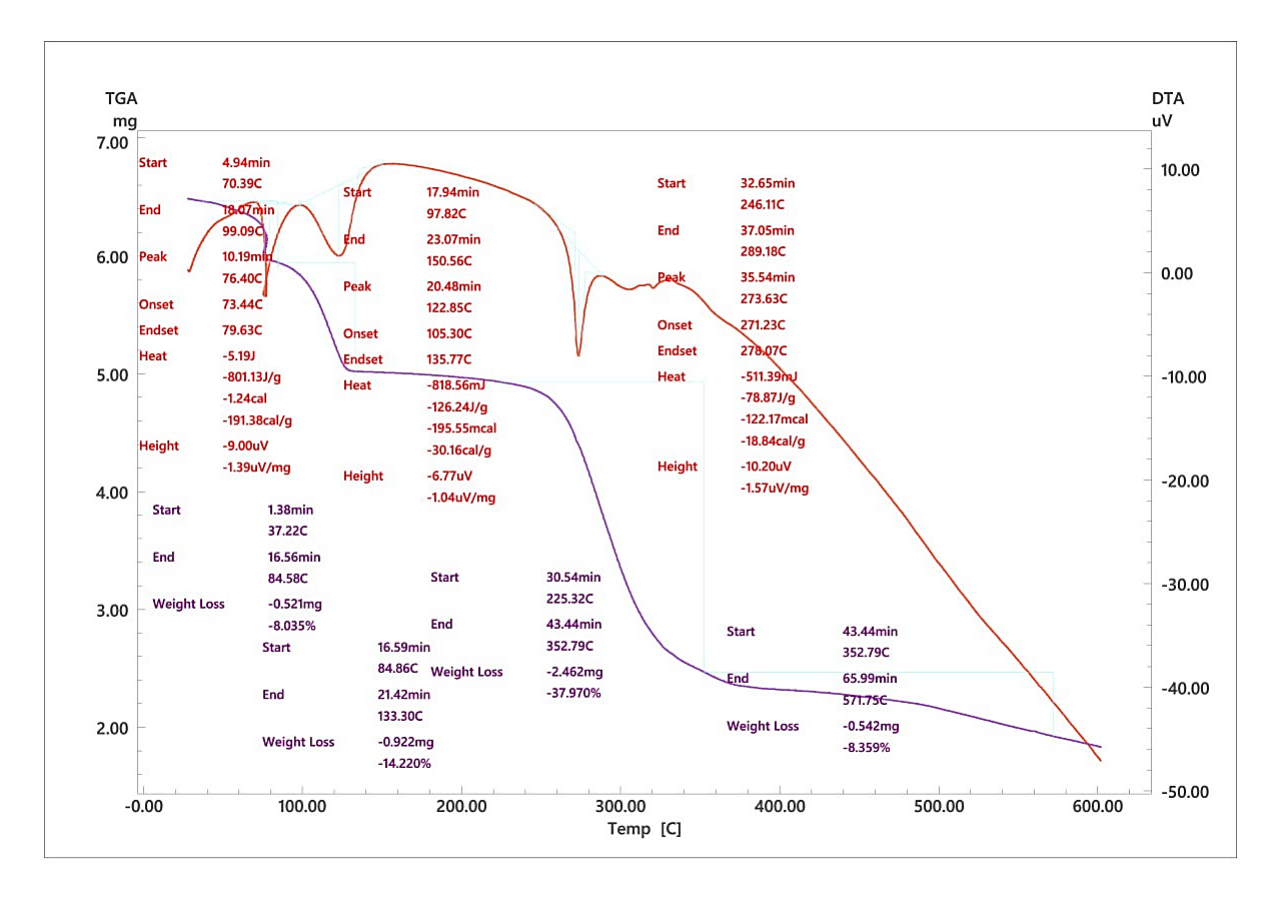


Figure 9. Thermogravimetric (TGA) and differential thermal analysis (DTA) of the [(CH-3COO)<sub>2</sub>(C<sub>12</sub>H<sub>8</sub>N<sub>2</sub>)<sub>2</sub>Cd](2CH<sub>3</sub>COOH·2H<sub>2</sub>O) complex.

An analysis of the thermogravimetric analysis (TGA) curve and the differential thermal analysis (DTA) curve is presented in Table 4 below. From the table, it is

evident that the highest mass loss occurs during the third decomposition interval, where 37.970% of the mass is lost.

Table 4.

### Analysis of the Thermogravimetric (TGA) Curve

Temperatura <sup>0</sup> C	Time, minut	Weight (mg)	Lost mass (%)
37,22-84,58	15,18	0,521	8,035
84,58–133,30	15,469	0,922	14,220
225,32-352,79	12,79	2,462	37,970
352,79–571,75°C	22,55	0,542	8,359

Table 5: Detailed Analysis of the Thermogravimetric Analysis (TGA) Curve and Differential Thermal Analysis (DTA) Curve

Table 5. Effect of Temperature on Weight Loss of [(CH<sub>3</sub>COO)<sub>2</sub>(C<sub>1</sub>,H<sub>8</sub>N<sub>2</sub>),Cd](2CH<sub>3</sub>COOH·2H<sub>2</sub>O) Complex Sample

№	dw 6,48	1/T	dw/dt	M.g	Mint	T <sup>0</sup> +K
1	5.92	0.0026	0.033	0.56	16.8	373
2	4.97	0.0021	0.056	1.51	26.8	473
3	3.84	0.0017	0.071	2.64	36.8	573
4	2.33	0.0014	0.088	4.15	46.8	673
5	2.20	0.0012	0.075	4.28	56.9	773
6	1.83	0.0011	0.067	4.65	69.3	895

The activation energy values for the process are provided for the complex sample [(CH<sub>3</sub>COO)2(C<sub>12</sub>H<sub>8</sub>N<sub>2</sub>)<sub>2</sub>Cd](2CH-<sub>3</sub>COOH·2H<sub>2</sub>O) in Table 6.

Results of Thermal-Oxidation Analysis of [(CH<sub>1</sub>COO)<sub>2</sub>(C<sub>1</sub>,H<sub>8</sub>N<sub>2</sub>),Cd](2·CH<sub>3</sub>COOH·2H<sub>2</sub>O) Complex Sample

№	dw 6.48	$Ln(W_1/W_2)$	1/T *10 <sup>-3</sup>
1	5.92	0.0904	2.6
2	4.97	0.2653	2.1
3	3.84	0.5234	1.7
4	2.33	1.0230	1.4
5	2.20	1.0802	1.2
6	1.83	1.2644	1.1

Based on the experimental data obtained on the kinetics of processes in the temperature range from 310.22 K to 844.75 K, the thermal oxidation characteristics and degradation behavior of the complex sample [(CH,COO),(C<sub>1</sub>,H<sub>o</sub>N<sub>2</sub>),Cd] (2CH,COOH·2H,O) were studied.

### Conclusion

For the first time, a complex compound containing  $[(CH_3COO)_2(C_{12}H_8N_2)_2Cd](2\cdot CH_3COOH\cdot 2H_2O)$  was synthesized and its molecular and crystal structure were determined by X-ray diffraction. In the Hirschfeld surface analysis of the complex, the majority of interactions are H...H (46.4%), O...H/H...O (25.9%), H...C/C...H (19.4%), C...C (5.8 %), H...N/N..H (1.8%), and O...C/C...O (0.7%) were found. Ligand and complex Raman and IR spectra analysis revealed significant changes in several absorption lines in the ligand's Raman and IR spectra during complex formation. For example, these changes may be attributed to the coordination of the two nitrogen atoms of phen with the metal ion, as observed in the IR spectra. In the complex, the bands at 491 cm-1 and 631 cm-1 can be assigned to the stretching vibrations of Cd-O and Cd-N bonds, respec-

Thermogravimetric analysis (TGA) and differential thermal analysis (DTA) were conducted to study the thermal-oxidative degradation characteristics in the temperature range from 310.22 K to 844.75 K.

### References

1. Nwokeke U. G., Peter C. L. Synthesis and characterization of cadmium (II) complexes of 1, 10 phenanthroline and purine //journal of chemical society of nigeria. - 2018. - T. 43. - Nº. 4. https://www.journals.chemsociety. org.ng/index.php/jcsn/article/view/215 2. Toshtemirov, A.E., Turaev, K.K., Umbarov, IA va boshqalar. Mandel kislotasi ishtirokida 1,10-fenantrolin va nitrat anioni bilan mis (II) kompleksining sintezi va bu kompleksning kristalli tuzilishi. Kristallogr. Rep. 69 1087-1092 (2024). https://doi.org/10.1134/ S1063774524602065 3. E, T. A.; KhKh, T.; AB, I.; IA, U.; JM, A.; BKh, A. A new mixed ligand Copper (II) complex: synthesis, crystal structure and Hirshfeld surface analysis. International Journal of Engineering Trends and Technology 2024, 11 (11), 106-116. https://doi. org/10.14445/22315381/ijett-v72i11p114. 4. Toshtemirov A.E., Turaev X.X., Ashurov J.M., Umbarov I.A., Djalilov.A.T, Synthesis and research of mixed ligand complexes of cobalt (II) and manganese (II) ions with



1,10-phenanthroline Vol. 3 No. 3.2.1 (2023) OʻzMU xabarlari http://journals. nuu.uz

5. Summaries M. C. et al. Mineral commodity summaries //US Geological Survey: Reston, VA, USA. – 2021. – T. 200..

6. Manohar A. et al. bis (di (2-hydroxyethyl) dithiocarbamato) cadmium (II) with N-donor ligands: Synthesis, spectra, thermal studies and bond valence sum (BVS) analysis //Int. J. Chem. Tech. Res. – 2012. – T. 4. – C. 1023-1032

7. Saghatforoush L. A. et al. Preparation of Zinc (II) and Cadmium (II) Complexes of the Tetradentate Schiff Base Ligand 2-((E)-(2-(2-(pyridine-2-yl)-ethylthio) ethylimino) methyl)-4-bromophenol (PytBrsaIH) //Molecules. – 2008. – T. 13. – Nº. 4. – C. 804-81l. https://www.mdpi.com/1420-3049/13/4/804#

8. Xcalibur. Oxford Difraction Ltd. CrysAlisPro. Version.1.171.33.44, 2009. 9. G. M. Sheldrick, "SHELXS-97 and SHELXL-97, Program for Crystal Struc ture Solution and Refinement" University of Gottingen, Gottingen, 1997.

1937.
10. C.F. Macrae, I.J. Bruno, J.A.
Chisholm, P.R. Edington, P. McCabe,
E. Pidcock, L. Rodriguez-Monge, R.
Taylor, J. van de Streek, P.A. Wood,
Mercury prog ram me// J Appl
Crystallogr.-2008. -41.-466-470.
11. Turner M. J., McKinnon J. J., Wolff
S. K., Grimwood D. J., Spackman
P. R., Jayatilaka D. & Spackman
M. A. (2017). CrystalExplorer17.5.
University of Western Australia. http://

energy frameworks: extension to metal coordination compounds, organic salts, solvates and open-shell systems //IUCrJ. - 2017. - T. 4. - №. 5. -C. 575-587 13. Kumara K. et al. Synthesis, crystal structure and 3D energy frameworks of ethyl 2-[5-nitro-2-oxopyridine-1 (2H)yl] acetate: Hirshfeld surface analysis and DFT calculations //Chemical Data Collections. - 2019. - T. 20. - C. 100195. 14. Zhu Z. Y., Gu R. A., Lu T. H. Application of Raman spectroscopy in Chemistry //Shenyang, China: Northeastern University Press. [Google Scholar]. – 1998. – C. 302-303. 15. Qizhuang H. et al. Studies on the spectra and antibacterial properties of rare earth dinuclear complexes with L-phenylalanine and o-phenanthroline //Materials letters. – 2006. - T. 60. - Nº. 3. - C. 317-320. 16. Shaabani B. et al. Sonochemical Synthesis of a Novel Nanoscale Lead (II) Coordination Polymer: Synthesis, Crystal Structure, Thermal Properties, and DFT Calculations of [Pb (dmp) (µ-N3)(µ-NO3)] n with the Novel Pb2 (μ-N3) 2 (μ-NO3) 2 Unit. – 2011. https:// doi.org/10.1002/zaac.201000426 17. Muratov, B. A., Turaev Kh Kh, and I. A. Umbarov. "Kasimov Sh. A, Nomozov AK," Studying of Complexes of Zn (II) and Co (II) with Acyclovir (2-amino-9-((2hydroxyethoxy) methyl)-1, 9-dihydro-6H-purine-6-OH),"." International Journal of Engineering Trends and Technology 72.1 (2024): 202-208.

CrystalExplorer model energies and